UC Irvine
UC Irvine Previously Published Works

Title

Ir(III)-Based Agents for Monitoring the Cytochrome P450 3A4 Active Site Occupancy.

Permalink

https://escholarship.org/uc/item/0w04q646

Journal

Inorganic Chemistry, 61(35)

Authors

Denison, Madeline
Steinke, Sean
Majeed, Aliza
et al.

Publication Date

2022-09-05

DOI

10.1021/acs.inorgchem.2c02587

Peer reviewed

eScholarship.org Powered by the California Digital Library
University of California

Author Manuscript
Author Manuscript
Author Manuscript
Author Manuscript

HHS Public Access
Author manuscript
Inorg Chem. Author manuscript; available in PMC 2023 September 05.

Published in final edited form as:
Inorg Chem. 2022 September 05; 61(35): 13673–13677. doi:10.1021/acs.inorgchem.2c02587.

Ir(III)-Based Agents for Monitoring the Cytochrome P450 3A4 Active Site Occupancy

Madeline Denison,
Department of Chemistry, Wayne State University, Detroit, Michigan 48202, United States

Sean J. Steinke,
Department of Chemistry and Biochemistry, The Ohio State University, Columbus, Ohio 43210, United States

Aliza Majeed,
Institute of Environmental Health Sciences, Wayne State University, Detroit, Michigan 48202, United States

Claudia Turro,
Department of Chemistry and Biochemistry, The Ohio State University, Columbus, Ohio 43210, United States;

Thomas A. Kocarek,
Institute of Environmental Health Sciences, Wayne State University, Detroit, Michigan 48202, United States;

Irina F. Sevrioukova,
Molecular Biology and Biochemistry, University of California, Irvine, California 92697, United States;

Jeremy J. Kodanko
Department of Chemistry, Wayne State University, Detroit, Michigan 48202, United States; Barbara Ann Karmanos Cancer Institute, Detroit, Michigan 48201,United States;

Abstract

Cytochromes P450 (CYPs) are a superfamily of enzymes responsible for biosynthesis and drug metabolism. Monitoring the activity of CYP3A4, the major human drug-metabolizing enzyme, is vital for assessing the metabolism of pharmaceuticals and identifying harmful drug–drug

Corresponding Authors: Claudia Turro − Department of Chemistry and Biochemistry, The Ohio State University, Columbus, Ohio 43210, United States; turro@chemistry.ohio-state.edu, **Thomas A. Kocarek** – Institute of Environmental Health Sciences, Wayne State University, Detroit, Michigan 48202, United States; t.kocarek@wayne.edu, **Irina F. Sevrioukova** – Molecular Biology and Biochemistry, University of California, Irvine, California 92697, United States; sevrioui@uci.edu, **Jeremy J. Kodanko** – Department of Chemistry, Wayne State University, Detroit, Michigan 48202, United States; Barbara Ann Karmanos Cancer Institute, Detroit, Michigan 48201,United States; jkodanko@chem.wayne.edu.

Supporting Information
The Supporting Information is available free of charge at https://pubs.acs.org/doi/10.1021/acs.inorgchem.2c02587.
Experimental procedures for the synthesis and spectral data for **2**–**5**, procedures for photophysical, pharmacological, and biological studies, and X-ray crystallographic data (PDF)

Complete contact information is available at: https://pubs.acs.org/10.1021/acs.inorgchem.2c02587

The authors declare no competing financial interest.

Author Manuscript Author Manuscript Author Manuscript Author Manuscript

interactions. Existing probes for CYP3A4 are irreversible turn-on substrates that monitor activity at specific time points in end-point assays. To provide a more dynamic approach, we designed, synthesized, and characterized emissive Ir(III) and Ru(II) complexes that allow monitoring of the CYP3A4 active-site occupancy in real time. In the bound state, probe emission is quenched by the active-site heme. Upon displacement from the active site by CYP3A4-specific inhibitors or substrates, these probes show high emission turn-on. Direct probe binding to the CYP3A4 active site was confirmed by X-ray crystallography. The lead Ir(III)-based probe has nanomolar K_d and high selectivity for CYP3A4, efficient cellular uptake, and low toxicity in CYP3A4-overexpressing HepG2 cells.

Cytochromes P450 (CYPs) are crucial enzymes responsible for biomolecule synthesis and drug metabolism. Among 57 human CYPs, CYP3A4 is the major drug-metabolizing enzyme responsible for oxidizing the majority of pharmaceuticals.[1] Because of high substrate promiscuity and plasticity of the active site, CYP3A4 is implicated in many drug–drug interactions that can cause drug toxicity.[2–5] Additionally, CYP3A4 displays genetic polymorphism, where mutations facilitate or slow down drug metabolism, thereby affecting the therapeutic efficiency.[6–8] These attributes make CYP3A4 an important target for activity monitoring, especially in complex systems such as liver microsomes and hepatocytes that model human drug metabolism *in vitro*. Current methods for monitoring CYP3A4 activity involve marker substrates, which require cumbersome and costly high-performance liquid chromatography analyses conducted over multiple time points, or irreversible turn-on reagents that make it difficult to monitor changes to CYP3A4 activity over time (Figure 1A).[9–14] As an alternative approach to these classical methods, in this Communication, we report emissive Ir(III) and Ru(II) complexes that allow sensing of the occupancy of the CYP3A4 active site (Figure 1B).

We chose to examine Ir(III) and Ru(II) complexes as probes for CYP3A4 because they are powerful tools for monitoring biological activity.[15–24] Probes of this class have long luminescence lifetimes, ranging from hundreds of nanoseconds up to ~100 μs,[15,16,25] which allows for time-resolved gating that can be used to exclude background emission from biomolecules and fluorogenic substrates. Thus, these compounds were expected to provide a distinct advantage over previous CYP3A4 probes containing organic-based fluorescent groups,[26] whose low nanosecond lifetimes preclude the measurement of CYP activity in human liver microsomes, the gold standard in drug metabolism.

Transition-metal-based probes were designed to interact with a hydrophobic surface within the substrate access channel of CYP3A4[27] and included a pyridyl side chain (see R_1 in Figure 2) to anchor the complex to the enzyme through direct heme iron coordination. Emissive sensors **2**–**5** were synthesized as racemic mixtures of Δ and Λ isomers (Figure 2A). Ligand **1** was heated with the Ru(II) precursors *cis*-$[Ru(L_1)_2Cl_2]$ (L_1 = 2,2′-bipyridine or 1,10-phenanthroline), which gave compounds **2** and **3**. Alternatively, treating **1** with $[Ir(\mu\text{-}Cl)(C\text{^}N)_2]_2$ [C^N = 2-phenylpyridine (ppy) or 2-phenylquinoline (pq)] gave complexes **4** and **5**. Complexes **2**–**5** were characterized by ^{1}H NMR, IR, and electronic absorption spectroscopies and electrospray ionization mass spectrometry. All data were consistent with the structures shown in Figure 2. Importantly, electronic absorption and emission spectra for

Author Manuscript Author Manuscript Author Manuscript Author Manuscript

2–**5** were in good agreement with data for the parent Ru(II) or Ir(III) complexes devoid of the R_1 side chain.[28–30] All complexes emit brightly when excited with 435 nm light (Figure S7), with **4** having the highest emission quantum yield of 0.086(9) and a lifetime of 1.6 μs, over twice as long as those of **2** and **3** (Table 1).

Equilibrium titration of CYP3A4 with **2**–**5** showed that all complexes exhibit type II binding, indicative of strong pyridine nitrogen coordination to the heme (Figure 3A,C–F). Spectral dissociation constants for **2**–**5** are listed in Table 1. Complexes **4** and **5** are far more potent than the Ru(II) inhibitors **2** and **3**, indicating that CYP3A4 preferably binds monocationic over dicationic complexes. Importantly, attachment of the R_1 side chain dramatically increases the inhibitory potency, by nearly 100-fold. The control compound **6** shows type I binding (a blue shift in the Soret band) and is a weak inhibitor with a K_d value of 11.2 ± 0.08 μM, whereas analogue **5** with the pyridyl-containing R_1 chain exhibits type II binding, with a stronger affinity of 130 ± 11 nM. Both the binding affinity determined from the equilibrium titrations and the IC_{50} data indicated that Ir(III) sensors bind tighter and inhibit CYP3A4 more potently than Ru(II) compounds, with tunable K_d values as low as 70 ± 2 nM for **4**.

Next, Ir(III) complexes **4** and **5** were cocrystallized with CYP3A4 (Figures 3C–F and S8). In both structures, the inhibitor's R_1 side chain curls above the heme and the terminal pyridine N ligates to the heme Fe (Fe–N distance of 2.20–2.23 Å). Hydrophobic residues Phe108, Phe220, Phe57, and Leu482 are in close contact with the ppy and pq groups of **4** and **5**, respectively. The electron density was well-defined for the heme-ligating pyridine, part of the tether, and the Ir(III) cores. The Ir ligands were poorly defined, which suggests that both the Δ and Λ isomers of **4** and **5** were bound to the active site. The stereochemistry was not specified during structural refinement, but the Λ and Δ isomers (shown in Figure 3C–F) were preferably selected for **4** and **5**, respectively, and fit into electron density maps by the refining program. Importantly, **4** and **5** are the first Ir complexes characterized to bind to a CYP enzyme.[31–38]

To ensure that **4** binds to CYP3A4 more selectively than to other CYP isoforms, the IC_{50} values of **4** against CYP3A4, CYP1A2, and CYP2C9 were determined using commercially available inhibitor screening kits (BioVision). Data from these kits versus the soluble reconstituted system in Table 1 cannot be compared directly because they were acquired under different conditions.[27] The derived IC_{50} values were 2.8 ± 1.0, >100, and 79 ± 6 μM for CYP3A4, CYP2C9, and CYP1A2, respectively (Figure 3G). The 28- and >36-fold difference in IC_{50} demonstrates the high selectivity and preferential binding of **4** to a larger and expandable active site of CYP3A4 (Figure S8). For comparison, the volume of the active-site cavity in ligand-free CYP3A4 is 1400 $Å^3$ relative to 375 and 470 $Å^3$ in CYP1A2 and CYP2C9, respectively.[7,39,40]

With compound **4** identified as a lead, we evaluated its ability to act as an active-site photosensor by measuring changes in emission intensity upon the addition of ligand-free or substrate/inhibitor-bound CYP3A4 (Figure 3H). Strong luminescence quenching was observed when **4** (5 μM) was mixed with ligand-free CYP3A4 (3 μM), consistent with other emissive probes for P450 enzymes.[41–45] The quenching was partial when CYP3A4

Author Manuscript Author Manuscript Author Manuscript Author Manuscript

was bound to a substrate or inhibitor prior to the addition of **4**. Importantly, the emission levels were ligand-dependent and correlated with the ligands' binding affinity: the strongest CYP3A4 binder, ritonavir (K_d = 19 nM), was the most difficult to displace, whereas the weakly bound substrate, testosterone (K_d of 1.5 and 30 μM for two binding sites), was expelled by the probe more easily.

To further substantiate the scope of our lead compound **4**, we assessed its inhibitory properties in HepG2 human hepatoma cells, where expression of most drug-metabolizing CYPs is negligible or absent. However, when HepG2 cells were stably engineered with vectors expressing CYPs, the protein levels reached those in primary human hepatocytes, which makes this model cell line a convenient *in vitro* tool to mimic drug metabolism in the liver.[46–48] To determine the CYP3A4 inhibitory activity of **4**, HepG2 cells overexpressing CYP3A4 were used in conjuction with a bioluminiscent P450-Glo CYP3A4 assay. Importantly, a strong concentration-dependent decrease in activity was observed, with statistically significant inhibition at 300 nM (Figure 3I; ~20% inhibition and $P < 0.05$ vs control). These data confirm that **4** is able to efficiently penetrate HepG2-CYP3A4 cells and inhibit CYP3A4 activity at nanomolar concentrations.

Finally, to demonstrate that our photosensors can be visualized in cells, we employed fluorescence microscopy. HepG2-CYP3A4 cells were treated with **4** (5 μM) for 1 h (Figure 3J), then rinsed with phosphate-buffered saline (PBS; pH 7.0), and imaged using the GFP channel. We found that **4** is cell-permeable and can be visually detected at concentrations as low as 5 μM. Utilization of metal complexes at such low concentrations limits their cell toxicity. In fact, **4** is well-tolerated by HepG2-CYP3A4 cells (EC_{50} > 50 μM), as judged by a cellular viability assay (Figure 3K, MTT, 72 h). This result provides strong evidence that cell toxicity can be avoided or largely minimized when Ir(III) complexes are used as photosensors at low concentrations (<10 μM).

In summary, Ir(III) compound **4** is a potent and specific inhibitor that serves as a photosensor for CYP3A4 active-site occupancy. The luminescence of **4** is quenched upon binding to CYP3A4 and recovers in a manner proportional to the binding affinity of CYP3A4 substrates and inhibitors. Furthermore, photosensor **4** penetrates and inhibits CYP3A4 in hepatic cells and emits brightly in the intracellular environment. This new class of photosensors is expected to provide a significant advantage over traditional end-point assays currently used for the detection of drug–drug interactions of CYP3A4 in cells. Another beneficial property of our photosensors is their prolonged luminescence lifetimes, which allow time-resolved emission measurements for excluding autofluorescence, a major problem in bioimaging that cannot be addressed with the current sensors. Studies are now underway in our laboratories to further develop this class of compounds and utilize Ir(III) photosensors for monitoring CYP3A4 active-site occupancy *in cellulo*.

Supplementary Material

Refer to Web version on PubMed Central for supplementary material.

Author Manuscript Author Manuscript Author Manuscript Author Manuscript

ACKNOWLEDGMENTS

We gratefully acknowledge the National Science Foundation (Grants CHE 2102508 and CHE 1764235), the National Institutes of Health (Grants ES025767 and T32GM142519), Richard Barber Interdisciplinary Research Program, and Wayne State University for support of this research. We thank Dr. Lei Guo of the National Center for Toxicology Research for generously providing HepG2-CYP3A4 cells. Part of our research was carried out at the Stanford Synchrotron Radiation Lightsource (SSRL) beamline 12-2. The SLAC National Accelerator Laboratory is supported by the U.S. Department of Energy (Grant DE-AC02-76SF00515). The SSRL Structural Molecular Biology Program is supported by the Department of Energy and National Institutes of Health (Grant P30GM133894).

REFERENCES

(1). Hodgson E In Vitro Human Phase I Metabolism of Xenobiotics I: Pesticides and Related Compounds Used in Agriculture and Public Health, May 2003. J. Biochem. Mol. Toxicol 2003, 17 (4), 201–206. [PubMed: 12898643]

(2). Chapman SA; Lake KD Considerations for Using Ketoconazole in Solid Organ Transplant Recipients Receiving Cyclosporine Immunosuppression. J. Transpl. Coord 1996, 6 (3), 7.

(3). van Eijk M; Boosman RJ; Schinkel AH; Huitema ADR; Beijnen JH Cytochrome P450 3A4, 3A5, and 2C8 Expression in Breast, Prostate, Lung, Endometrial, and Ovarian Tumors: Relevance for Resistance to Taxanes. Cancer Chemother. Pharmacol 2019, 84 (3), 487–499. [PubMed: 31309254]

(4). Brayer SW; Reddy KR Ritonavir-Boosted Protease Inhibitor Based Therapy: A New Strategy in Chronic Hepatitis C Therapy. Expert Rev. Gastroenterol. Hepatol 2015, 9 (5), 547–558. [PubMed: 25846301]

(5). Kempf DJ; Marsh KC; Kumar G; Rodrigues AD; Denissen JF; McDonald E; Kukulka MJ; Hsu A; Granneman GR; Baroldi PA; Sun E; Pizzuti D; Plattner JJ; Norbeck DW; Leonard JM Pharmacokinetic Enhancement of Inhibitors of the Human Immunodeficiency Virus Protease by Coadministration with Ritonavir. Antimicrob. Agents Chemother 1997, 41 (3), 654–660. [PubMed: 9056009]

(6). Lynch T; Price A The Effect of Cytochrome P450 Metabolism on Drug Response, Interactions, and Adverse Effects. Am. Fam. Physician 2007, 76 (3), 6.

(7). Zanger UM; Schwab M Cytochrome P450 Enzymes in Drug Metabolism: Regulation of Gene Expression, Enzyme Activities, and Impact of Genetic Variation. Pharmacol. Ther 2013, 138 (1), 103–141. [PubMed: 23333322]

(8). Johansson I; Ingelman-Sundberg M Genetic Polymorphism and Toxicology With Emphasis on Cytochrome P450. Toxicol. Sci 2011, 120 (1), 1–13. [PubMed: 21149643]

(9). Sevrioukova IF; Poulos TL Current Approaches for Investigating and Predicting Cytochrome P450 3A4–Ligand Interactions. In Monooxygenase, Peroxidase and Peroxygenase Properties and Mechanisms of Cytochrome P450; Hrycay EG, Bandiera SM, Eds.; Advances in Experimental Medicine and Biology; Springer International Publishing: Cham, Switzerland, 2015; Vol. 851, pp 83–105. DOI: 10.1007/978-3-319-16009-2_3.

(10). Raunio H; Pentikäinen O; Juvonen RO Coumarin-Based Profluorescent and Fluorescent Substrates for Determining Xeno-biotic-Metabolizing Enzyme Activities In Vitro. Int. J. Mol. Sci 2020, 21 (13), 4708.

(11). Ning J; Liu T; Dong P; Wang W; Ge G; Wang B; Yu Z; Shi L; Tian X; Huo X; Feng L; Wang C; Sun C; Cui J; James TD; Ma X Molecular Design Strategy to Construct the Near-Infrared Fluorescent Probe for Selectively Sensing Human Cytochrome P450 2J2. J. Am. Chem. Soc 2019, 141 (2), 1126–1134. [PubMed: 30525564]

(12). Dai Z-R; Ge G-B; Feng L; Ning J; Hu L-H; Jin Q; Wang D-D; Lv X; Dou T-Y; Cui J-N; Yang L A Highly Selective Ratiometric Two-Photon Fluorescent Probe for Human Cytochrome P450 1A. J. Am. Chem. Soc 2015, 137 (45), 14488–14495. [PubMed: 26488456]

(13). Ning J; Tian Z; Wang B; Ge G; An Y; Hou J; Wang C; Zhao X; Li Y; Tian X; Yu Z; Huo X; Sun C; Feng L; Cui J; Ma X A Highly Sensitive and Selective Two-Photon Fluorescent Probe for Real-Time Sensing of Cytochrome P450 1A1 in Living Systems. Mater. Chem. Front 2018, 2 (11), 2013–2020.

Author Manuscript Author Manuscript Author Manuscript Author Manuscript

(14). Dai Z-R; Feng L; Jin Q; Cheng H; Li Y; Ning J; Yu Y; Ge G-B; Cui J-N; Yang L A Practical Strategy to Design and Develop an Isoform-Specific Fluorescent Probe for a Target Enzyme: CYP1A1 as a Case Study. Chem. Sci 2017, 8 (4), 2795–2803. [PubMed: 28553516]

(15). Martí AA Metal Complexes and Time-Resolved Photoluminescence Spectroscopy for Sensing Applications. J. Photochem. Photobiol. Chem 2015, 307–308, 35–47.

(16). Huang K; Jiang C; Martí AA Ascertaining Free Histidine from Mixtures with Histidine-Containing Proteins Using Time-Resolved Photoluminescence Spectroscopy. J. Phys. Chem. A 2014, 118 (45), 10353–10358. [PubMed: 25313943]

(17). Lampe JN; Atkins WM Time-Resolved Fluorescence Studies of Heterotropic Ligand Binding to Cytochrome P450 3A4 †. Biochemistry 2006, 45 (40), 12204–12215. [PubMed: 17014074]

(18). Sreedharan S; Sinopoli A; Jarman PJ; Robinson D; Clemmet C; Scattergood PA; Rice CR; Smythe CGW; Thomas JA; Elliott PIP Mitochondria-Localising DNA-Binding Biscyclometalated Phenyltriazole Iridium(III) Dipyridophenazene Complexes: Syntheses and Cellular Imaging Properties. Dalton Trans. 2018, 47 (14), 4931–4940. [PubMed: 29552680]

(19). Liu H-W; Law WH-T; Lee LC-C; Lau JC-W; Lo KK-W Cyclometalated Iridium(III) Bipyridine-Phenylboronic Acid Complexes as Bioimaging Reagents and Luminescent Probes for Sialic Acids. Chem. - Asian J 2017, 12 (13), 1545–1556. [PubMed: 28418182]

(20). Wang W; Lu L; Wu K-J; Liu J; Leung C-H; Wong C-Y; Ma D-L Long-Lived Iridium(III) Complexes as Luminescent Probes for the Detection of Periodate in Living Cells. Sens. Actuators B Chem 2019, 288, 392–398.

(21). Zhang C; Qiu K; Liu C; Huang H; Rees TW; Ji L; Zhang Q; Chao H Tracking Mitochondrial Dynamics during Apoptosis with Phosphorescent Fluorinated Iridium(III) Complexes. Dalton Trans. 2018, 47 (37), 12907–12913. [PubMed: 30117504]

(22). Wu X; Zheng Y; Wang F; Cao J; Zhang H; Zhang D; Tan C; Ji L; Mao Z Anticancer Ir^{III} − Aspirin Conjugates for Enhanced Metabolic Immuno-Modulation and Mitochondrial Lifetime Imaging. Chem. Eur. J 2019, 25 (28), 7012–7022. [PubMed: 30913329]

(23). Shaikh S; Wang Y; ur Rehman F; Jiang H; Wang X Phosphorescent Ir (III) Complexes as Cellular Staining Agents for Biomedical Molecular Imaging. Coord. Chem. Rev 2020, 416, 213344.

(24). Cook NP; Torres V; Jain D; Martí AA Sensing Amyloid-β Aggregation Using Luminescent Dipyridophenazine Ruthenium(II) Complexes. J. Am. Chem. Soc 2011, 133 (29), 11121–11123. [PubMed: 21714574]

(25). Huang K; Bulik IW; Martí AA Time-Resolved Photoluminescence Spectroscopy for the Detection of Cysteine and Other Thiol Containing Amino Acids in Complex Strongly Autofluorescent Media. Chem. Commun 2012, 48 (96), 11760.

(26). Chougnet A; Grinkova Y; Ricard D; Sligar S; Woggon W-D Fluorescent Probes for Rapid Screening of Potential Drug–Drug Interactions at the CYP3A4 Level. ChemMedChem. 2007, 2 (5), 717–724. [PubMed: 17357170]

(27). Toupin N; Steinke SJ; Nadella S; Li A; Rohrabaugh TN; Samuels ER; Turro C; Sevrioukova IF; Kodanko JJ Photosensitive Ru(II) Complexes as Inhibitors of the Major Human Drug Metabolizing Enzyme CYP3A4. J. Am. Chem. Soc 2021, 143 (24), 9191–9205. [PubMed: 34110801]

(28). Kwon T-H; Oh YH; Shin I-S; Hong J-I New Approach Toward Fast Response Light-Emitting Electrochemical Cells Based on Neutral Iridium Complexes via Cation Transport. Adv. Funct. Mater 2009, 19 (5), 711–717.

(29). Wu S-H; Ling J-W; Lai S-H; Huang M-J; Cheng CH; Chen I-C Dynamics of the Excited States of $[Ir(Ppy)_2 Bpy]^+$ with Triple Phosphorescence. J. Phys. Chem. A 2010, 114 (38), 10339–10344. [PubMed: 20809643]

(30). Bouskila A; Drahi B; Amouyal E; Sasaki I; Gaudemer A Mononuclear and Binuclear Ruthenium(II) Heteroleptic Complexes Based on 1,10-Phenanthroline Ligands. J. Photochem. Photobiol. Chem 2004, 163 (3), 381–388.

(31). Wu S; Zhou Y; Rebelein JG; Kuhn M; Mallin H; Zhao J; Igareta NV; Ward TR Breaking Symmetry: Engineering Single-Chain Dimeric Streptavidin as Host for Artificial Metalloenzymes. J. Am. Chem. Soc 2019, 141 (40), 15869–15878. [PubMed: 31509711]

Author Manuscript Author Manuscript Author Manuscript Author Manuscript

(32). Feng L; Geisselbrecht Y; Blanck S; Wilbuer A; Atilla-Gokcumen GE; Filippakopoulos P; Kräling K; Celik MA; Harms K; Maksimoska J; Marmorstein R; Frenking G; Knapp S; Essen L-O; Meggers E Structurally Sophisticated Octahedral Metal Complexes as Highly Selective Protein Kinase Inhibitors. J. Am. Chem. Soc 2011, 133 (15), 5976–5986. [PubMed: 21446733]

(33). Rebelein JG; Cotelle Y; Garabedian B; Ward TR Chemical Optimization of Whole-Cell Transfer Hydrogenation Using Carbonic Anhydrase as Host Protein. ACS Catal. 2019, 9 (5), 4173–4178. [PubMed: 31080690]

(34). Monnard FW; Nogueira ES; Heinisch T; Schirmer T; Ward TR Human Carbonic Anhydrase II as Host Protein for the Creation of Artificial Metalloenzymes: The Asymmetric Transfer Hydrogenation of Imines. Chem. Sci 2013, 4 (8), 3269.

(35). Sullivan MP; Cziferszky M; Tolbatov I; Truong D; Mercadante D; Re N; Gust R; Goldstone DC; Hartinger CG Probing the Paradigm of Promiscuity for N-Heterocyclic Carbene Complexes and Their Protein Adduct Formation. Angew. Chem., Int. Ed 2021, 60 (36), 19928–19932.

(36). Robles VM; Dürrenberger M; Heinisch T; Lledós A; Schirmer T; Ward TR; Maréchal J-D Structural, Kinetic, and Docking Studies of Artificial Imine Reductases Based on Biotin–Streptavidin Technology: An Induced Lock-and-Key Hypothesis. J. Am. Chem. Soc 2014, 136 (44), 15676–15683. [PubMed: 25317660]

(37). Heinisch T; Pellizzoni M; Dürrenberger M; Tinberg CE; Köhler V; Klehr J; Häussinger D; Baker D; Ward TR Improving the Catalytic Performance of an Artificial Metalloenzyme by Computational Design. J. Am. Chem. Soc 2015, 137 (32), 10414–10419. [PubMed: 26226626]

(38). Stein A; Chen D; Igareta NV; Cotelle Y; Rebelein JG; Ward TR A Dual Anchoring Strategy for the Directed Evolution of Improved Artificial Transfer Hydrogenases Based on Carbonic Anhydrase. ACS Cent. Sci 2021, 7 (11), 1874–1884. [PubMed: 34849402]

(39). Yano JK; Wester MR; Schoch GA; Griffin KJ; Stout CD; Johnson EF The Structure of Human Microsomal Cytochrome P450 3A4 Determined by X-Ray Crystallography to 2.05-Å Resolution. J. Biol. Chem 2004, 279 (37), 38091–38094. [PubMed: 15258162]

(40). Williams PA; Cosme J; Ward A; Angove HC; Matak Vinković D; Jhoti H Crystal Structure of Human Cytochrome P450 2C9 with Bound Warfarin. Nature 2003, 424 (6947), 464–468. [PubMed: 12861225]

(41). Hays A-MA; Dunn AR; Chiu R; Gray HB; Stout CD; Goodin DB Conformational States of Cytochrome P450cam Revealed by Trapping of Synthetic Molecular Wires. J. Mol. Biol 2004, 344 (2), 455–469. [PubMed: 15522298]

(42). Dunn AR; Hays A-MA; Goodin DB; Stout CD; Chiu R; Winkler JR; Gray HB Fluorescent Probes for Cytochrome P450 Structural Characterization and Inhibitor Screening. J. Am. Chem. Soc 2002, 124 (35), 10254–10255. [PubMed: 12197708]

(43). Dmochowski IJ; Crane BR; Wilker JJ; Winkler JR; Gray HB Optical Detection of Cytochrome P450 by Sensitizer-Linked Substrates. PNAS 1999, 96 (23), 12987–12990. [PubMed: 10557259]

(44). Dunn AR; Dmochowski IJ; Bilwes AM; Gray HB; Crane BR Probing the Open State of Cytochrome P450cam with Ruthenium-Linker Substrates. Proc. Natl. Acad. Sci. U. S. A 2001, 98 (22), 12420–12425. [PubMed: 11606730]

(45). Contakes SM; Juda GA; Langley DB; Halpern-Manners NW; Duff AP; Dunn AR; Gray HB; Dooley DM; Guss JM; Freeman HC Reversible Inhibition of Copper Amine Oxidase Activity by Channel-Blocking Ruthenium(II) and Rhenium(I) Molecular Wires. Proc. Natl. Acad. Sci. U.S.A 2005, 102 (38), 13451–6. [PubMed: 16157884]

(46). Chen S; Wu Q; Li X; Li D; Mei N; Ning B; Puig M; Ren Z; Tolleson WH; Guo L Characterization of Cytochrome P450s (CYP)-Overexpressing HepG2 Cells for Assessing Drug and Chemical-Induced Liver Toxicity. J. Environ. Sci. Health Part C 2021, 39 (1), 68–86.

(47). Xuan J; Chen S; Ning B; Tolleson WH; Guo L Development of HepG2-Derived Cells Expressing Cytochrome P450s for Assessing Metabolism-Associated Drug-Induced Liver Toxicity. Chem. Biol. Interact 2016, 255, 63–73. [PubMed: 26477383]

(48). Yoshitomi S; Ikemoto K; Takahashi J; Miki H; Namba M; Asahi S Establishment of the Transformants Expressing Human Cytochrome P450 Subtypes in HepG2, and Their Applications on Drug Metabolism and Toxicology. Toxicol. In Vitro 2001, 15 (3), 245–256. [PubMed: 11377097]

Author Manuscript Author Manuscript Author Manuscript Author Manuscript

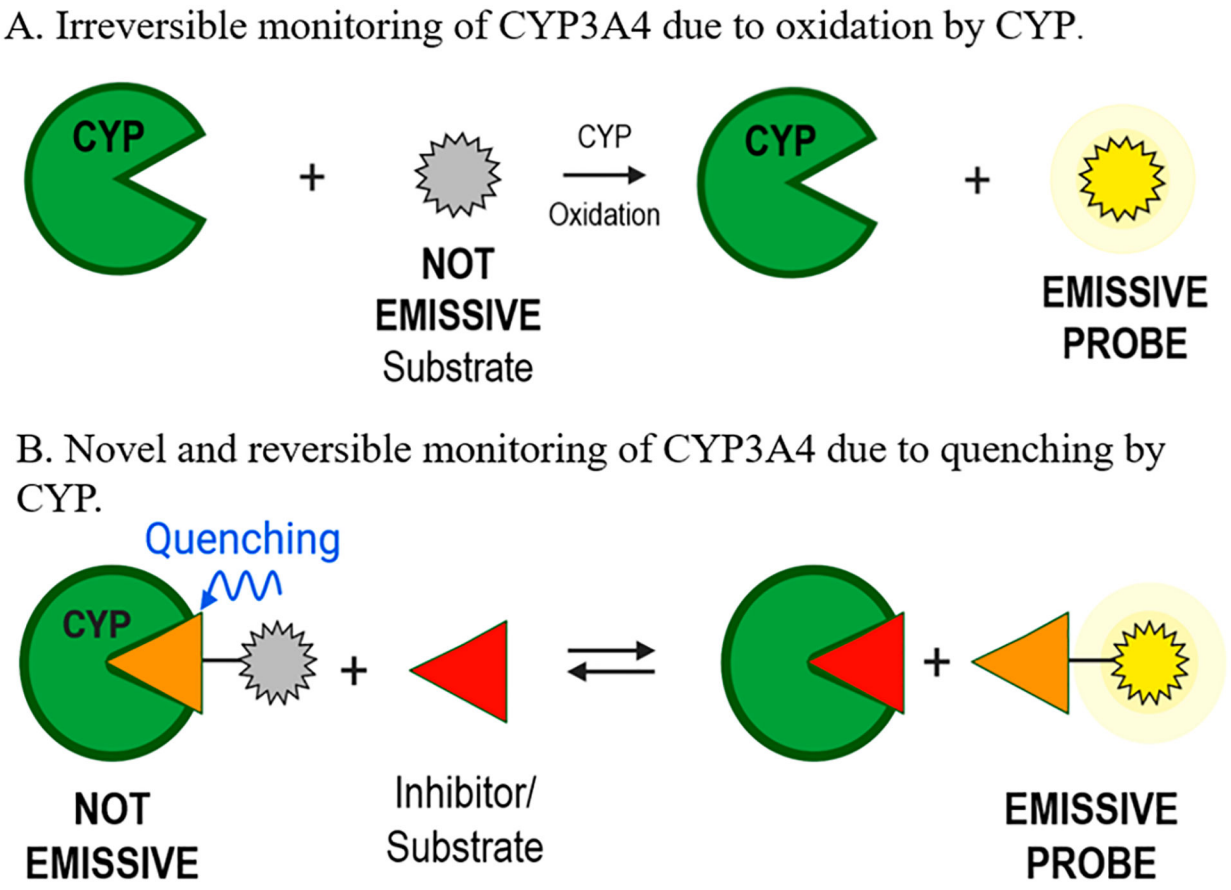

Figure 1.
Emissive probes for monitoring metabolism by CYP3A4.

Author Manuscript Author Manuscript Author Manuscript Author Manuscript

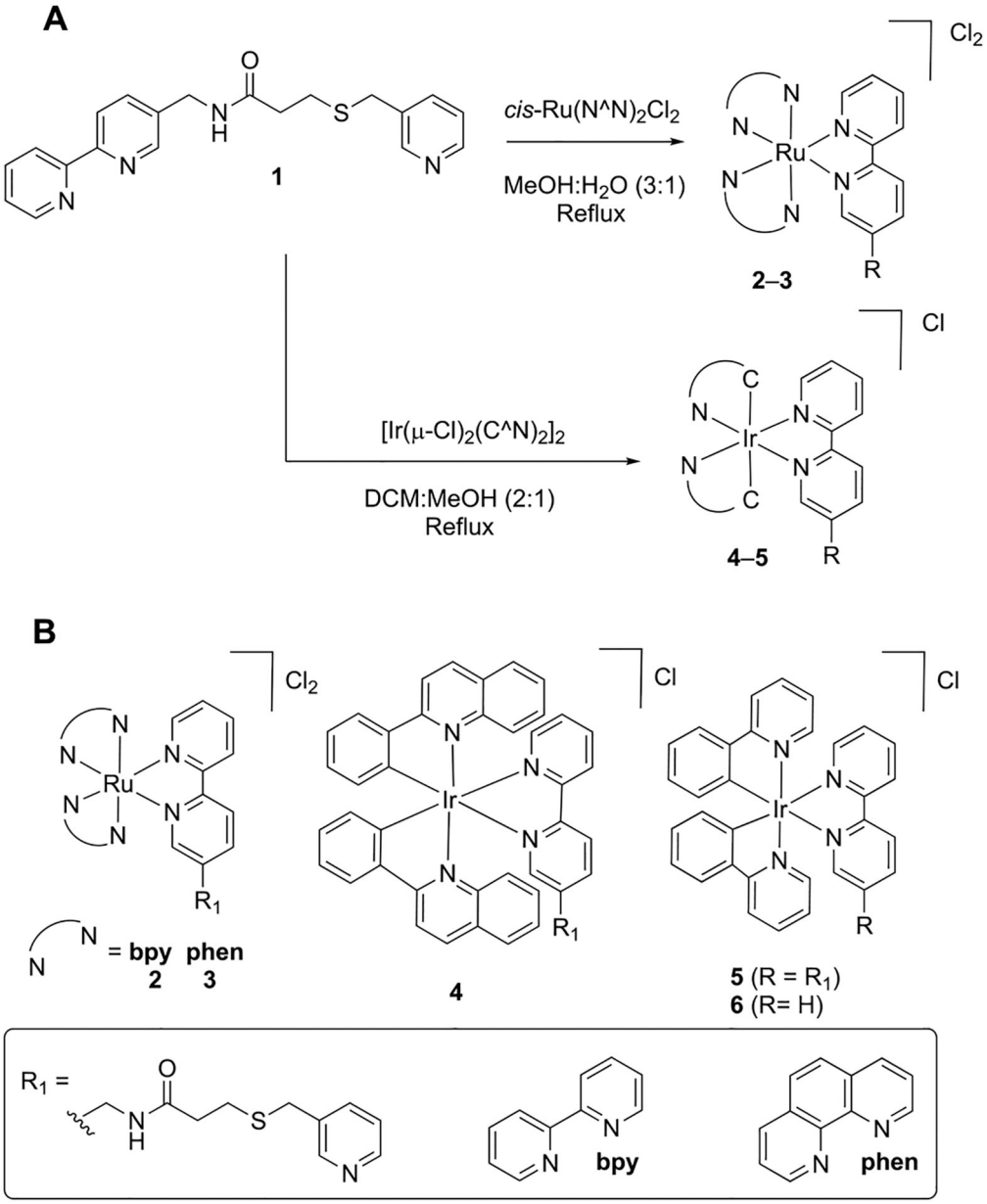

Figure 2.

Synthesis (A) and structures (B) of the Ir(III) and Ru(II) CYP3A4 photosensors **2**–**5**.

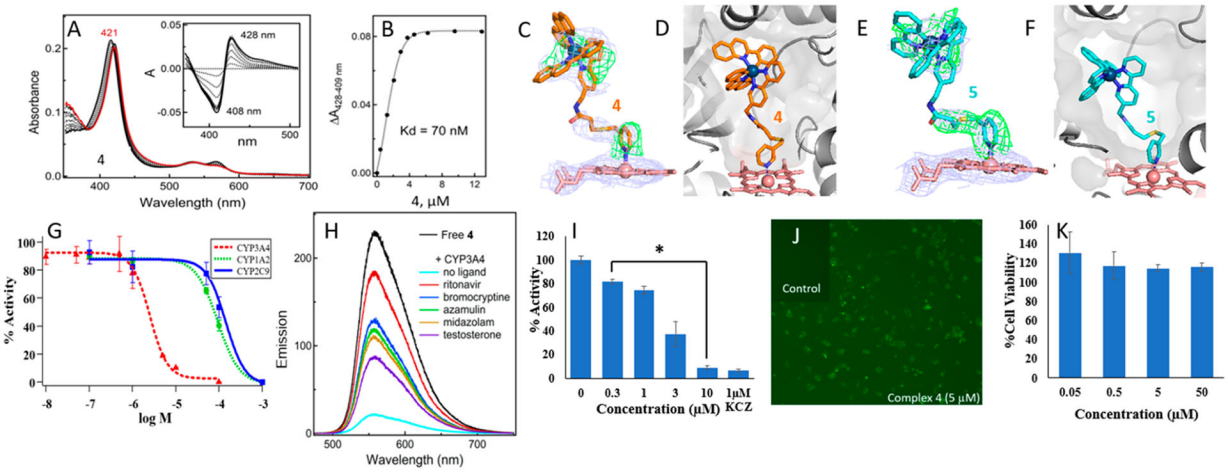

Figure 3.

(A) Spectral changes observed during equilibrium titration of CYP3A4 with **4**. The inset contains difference spectra. (B) Titration plot with the derived K_d values. (C and D) Crystal structure of the **4**–CYP3A4 complex at 2.78 Å resolution (PDB 7UAY). (E and F) Crystal structure of the **5**-CYP3A4 complex at 2.65 Å resolution (PDB 7UAZ). The blue and green meshes in panels C and E are $2F_o - F_c$ and polder-omit electron density maps contoured at the 1σ and 3σ levels, respectively. (G) Inhibition of CYP3A4, CYP1A4, and CYP2C9 activity by **4**. (H) Fluorescence spectra of **4** (5 μM) in the absence and presence of CYP3A4 (3 μM) bound to different substrates and inhibitors (10–20 μM) showing ligand-dependent emission yields (0.1 M PBS, pH 7.4, 10% glycerol, and λ_{ex} = 433 nm). (I) CYP3A4 activity with **4** (0.3–10 μM) determined by P450-Glo CYP3A4 assay or ketoconazole (1 μM) as a positive control. Concentrations of 0.3–10 μM are statistically significant from a control-containing vehicle: *, $P < 0.05$. (J) Fluorescence microscopy image (GFP filter) of HepG2-CYP3A4 cells treated with **4** (5 μM). The inset is control fluorescence from vehicle-treated cells. (K) Cell viability at different concentrations of **4** (0.05–50 μM) determined by a cellular viability assay (MTT, 72 h).

Author Manuscript Author Manuscript Author Manuscript Author Manuscript

Author Manuscript

Author Manuscript

Author Manuscript

Author Manuscript

Table 1.

Dissociation Constants (K_d), IC_{50} Values for CYP3A4 (μM), and Emission Quantum Yields for Sensors 2–5

			H_2O	
compound	K_d[a] (μM)	IC_{50}[b] (μM)	Φ_{em}[c]	τ (μs)
2	53 ± 4	6.0 ± 0.5	0.046(3)	0.66
3	23 ± 2	3.1 ± 0.4	0.042(9)	0.75
4	0.070 ± 0.0.002	0.25 ± 0.02	0.086(9)	1.6
5	0.130 ± 0.011	0.20 ± 0.01	0.007(1)	0.062
6	11.2 ± 0.8	1.02 ± 0.02	ND	ND

[a]Determined by spectrophotometric titration assay.

[b]CYP3A4 activity assay with BFC, 293 ± 3 K, 0.2 μM CYP3A4, 0.3 μM cytochrome P450 reductase, versus DMSO control (100% activity), and standard error <10%.

[c]Emission spectra of absorption matched solutions in Arsparged H_2O (A_{435} ~ 0.07), with λ_{ex} = 435 nm, a 455 nm long-pass filter, referenced to $Ru(bpy)_3$, and Φ_{em} = 0.042.